

## Double-Bridge Bonding of Aluminium and Hydrogen in the Crystal Structure of $\gamma$ -AlH<sub>3</sub>

Volodymyr A. Yartys,<sup>\*,†</sup> Roman V. Denys,<sup>†</sup> Jan Petter Maehlen,<sup>†</sup> Christoph Frommen,<sup>‡</sup> Maximilian Fichtner,<sup>‡</sup> Boris M. Bulychev,<sup>§</sup> and Hermann Emerich<sup>#</sup>

*Institute for Energy Technology, Kjeller NO 2027, Norway, Institute of Nanotechnology, Forschungszentrum Karlsruhe GmbH, P.O. Box 30640, D-76021 Karlsruhe, Germany, Chemistry Department, Moscow State University, Leninskie Gori, Moscow 119992, Russia, and Swiss-Norwegian Beam Line, ESRF, BP 220, F-38043 Grenoble, France*

Received September 14, 2006

Aluminum trihydride (alane) is one of the most promising among the prospective solid hydrogen-storage materials, with a high gravimetric and volumetric density of hydrogen. In the present work, the alane, crystallizing in the  $\gamma$ -AlH<sub>3</sub> polymorphic modification, was synthesized and then structurally characterized by means of synchrotron X-ray powder diffraction. This study revealed that  $\gamma$ -AlH<sub>3</sub> crystallizes with an orthorhombic unit cell (space group *Pnmm*,  $a = 5.3806(1)$  Å,  $b = 7.3555(2)$  Å,  $c = 5.77509(5)$  Å). The crystal structure of  $\gamma$ -AlH<sub>3</sub> contains two types of AlH<sub>6</sub> octahedra as the building blocks. The Al–H bond distances in the structure vary in the range of 1.66–1.79 Å. A prominent feature of the crystal structure is the formation of the bifurcated *double-bridge* bonds, Al–2H–Al, in addition to the normal bridge bonds, Al–H–Al. This former feature has not been previously reported for Al-containing hydrides so far. The geometry of the double-bridge bond shows formation of short Al–Al (2.606 Å) and Al–H (1.68–1.70 Å) bonds compared to the Al–Al distances in Al metal (2.86 Å) and Al–H distances for Al atoms involved in the formation of normal bridge bonds (1.769–1.784 Å). The crystal structure of  $\gamma$ -AlH<sub>3</sub> contains large cavities between the AlH<sub>6</sub> octahedra. As a consequence, the density is 11% less than for  $\alpha$ -AlH<sub>3</sub>.

### Introduction

Aluminum trihydride (alane), having a high gravimetric (10 wt %) and volumetric density of hydrogen (twice that of liquid H<sub>2</sub>), is among the most promising materials for on-board hydrogen-storage applications.

An ethereal complex of solvated alane was first synthesized in 1947 by an exchange reaction between AlCl<sub>3</sub> and lithium hydride in ether solution.<sup>1</sup> Its synthesis in nonsolvated form was first described in ref 2. AlH<sub>3</sub> forms six polymorphic modifications,  $\alpha$ ,  $\alpha'$ ,  $\beta$ ,  $\gamma$ ,  $\delta$ , and  $\epsilon$ , which are considered to be polymers (AlH<sub>3</sub>)<sub>*n*</sub>.<sup>2</sup> The measured thermodynamic properties of alane show that the equilibrium hydrogen pressure in

the Al–AlH<sub>3</sub> system is extremely high at ambient temperatures exceeding 25 kBar; therefore, alane should easily decompose at normal conditions and can be only formed by application of extremely high hydrogen pressures.<sup>3,4</sup> However, AlH<sub>3</sub> does not release very much hydrogen even while storing for years because the decomposition is kinetically hindered, possibly because of the formation of a thin protective oxide layer.

At atmospheric pressure, AlH<sub>3</sub> desorbs hydrogen at rather moderate temperatures (350–400 K, depending on its preparation history). Sufficiently rapid and controllable decomposition of AlH<sub>3</sub> and efficient synthesis routes to make the Al–AlH<sub>3</sub> system reversible are focuses in ongoing research (see, for example, ref 5). The doping of alane with LiH assists in solving the first task. All other alane modifications, including  $\gamma$ -alane, are less stable than  $\alpha$ -alane

\* To whom correspondence should be addressed. E-mail: Volodymyr.Yartys@ife.no. Phone: +47 63 80 64 53. Fax: +47 63 81 29 05.

<sup>†</sup> Institute for Energy Technology.

<sup>‡</sup> Institute of Nanotechnology, Forschungszentrum Karlsruhe GmbH.

<sup>§</sup> Moscow State University.

<sup>#</sup> Swiss-Norwegian Beam Line.

(1) Finholt, A. E.; Bond, C., Jr.; Schlesinger, H. I. *J. Amer. Chem. Soc.* **1947**, *69*, 1199–1203.

(2) Brower, F. M.; Matzek, N. E.; Reigler, P. F.; Rinn, H. W.; Roberts, C. B.; Schmidt, D. L.; Snover, J. A.; Terada, K. *J. Amer. Chem. Soc.* **1976**, *98*, 2450–2453.

(3) (a) Tkacz, M.; Filipek, S.; Baranowski, B. *Pol. J. Chem.* **1983**, *57*, 651–653. (b) Baranowski, B.; Tkacz, M. *Z. Phys. Chem.* **1983**, *135*, 27.

(4) Kononov, S. K.; Bulychev, B. M. *Inorg. Chem.* **1995**, *34*, 172.

(5) Sandrock, G.; Reilly, J. J.; Graetz, J.; Zhou, W.-M.; Johnson, J.; Wegrzyn, J. *Appl. Phys. A* **2005**, *80*, 687–690.

and transform into the  $\alpha$ -modification at temperatures slightly above ambient.<sup>6</sup>

$\alpha$ -AlH<sub>3</sub> is the best-studied modification of alane. These studies included its structural characterization.<sup>7,8</sup> The high-resolution synchrotron X-ray diffraction (SR-XRD) structural study<sup>8</sup> showed that a rhombohedral lattice of  $\alpha$ -AlH<sub>3</sub> (space group  $R\bar{3}c$ ,  $a = 4.44994(5)$  Å,  $c = 11.8200(2)$  Å,  $V = 202.701(4)$  Å<sup>3</sup>) is composed of vertex-sharing AlH<sub>6</sub> octahedra. The Al–H–Al bridge bonds are formed and have the following characteristics:  $\angle\text{Al–H–Al} = 142.0(7)^\circ$ ,  $d_{\text{Al–H}} = 1.712(3)$  Å. The refinements of the diffraction data indicated a small charge transfer from Al to H, corresponding to the formation of Al<sup>+0.15</sup> and H<sup>-0.05</sup>.

However, the structures of the other allotropic modifications of the alane have not been reported yet. The present paper gives results of the studies of the crystal structure of  $\gamma$ -AlH<sub>3</sub> by means of SR-XRD.

## Experimental Section

Synthesis of  $\gamma$ -alane was performed by two different groups, the Institute of Nanotechnology, FZK, in Germany (M.F. and C.F.) and Moscow State University in Russia (B.M.B.). Both synthesis techniques, despite differences in the synthesis processes, resulted in obtaining a nearly single-phase  $\gamma$ -AlH<sub>3</sub>. For further studies, by SR-XRD, the sample prepared at FZK was used. However, both synthesis routes will be described below.

### Synthesis at Institute of Nanotechnology, FZK. Reagents.

Diethyl ether (Merck, certified ACS, 99% purity) was double-distilled over sodium/benzophenone and LiAlH<sub>4</sub> and stored under purified nitrogen. AlCl<sub>3</sub> (Merck, anhydrous, >98%) was used as received. LiAlH<sub>4</sub> (Merck, >97%) was purified prior to use by dissolution in DEE and filtration of a light gray residue. After the solvent was evaporated under a vacuum, a white powder was obtained. According to powder XRD measurements, the material was purely a single phase.

Chemical synthesis of  $\gamma$ -AlH<sub>3</sub> was carried out on the bench using Schlenk tube techniques. The glassware was evacuated down to a pressure of 10<sup>-3</sup> mbar and flushed with dry oxygen-free nitrogen prior to use. Solids were handled in an argon-filled glove box equipped with a recirculation and regeneration system. Both the water and oxygen concentrations were kept below 1 ppm during operation. The synthesis procedure is a modification of a description given in the literature.<sup>1</sup>

Diethyl ether solutions of LiAlH<sub>4</sub> (2.4 g, 250 mL of Et<sub>2</sub>O) and AlCl<sub>3</sub> (2.1 g, 70 mL of Et<sub>2</sub>O) were prepared; both were precooled in an ice bath, and the AlCl<sub>3</sub> solution was quickly added to the LiAlH<sub>4</sub> solution with stirring. The reaction proceeded immediately, forming a fine, white precipitate. Stirring was continued for a period of 5 min; the precipitate was allowed to settle, and the solution was filtered through a fine grade glass filter frit into a round-bottom flask fitted with a nitrogen inlet. After filtration, the solvent was slowly removed at room temperature under vacuum (10<sup>-3</sup> mbar), and the remaining white residue was ground and heated under vacuum at 60 °C in a rotating glass oven (Büchi B585) for 4 h.

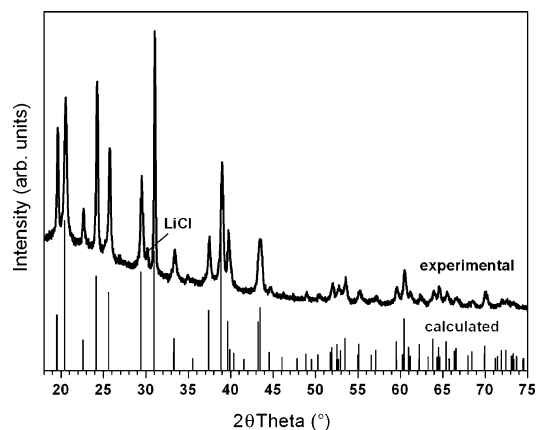


**Figure 1.** Experimental and calculated powder XRD pattern of  $\gamma$ -AlH<sub>3</sub> (Cu K $\alpha$ ). The calculation was performed on the basis of the structural data of this paper.

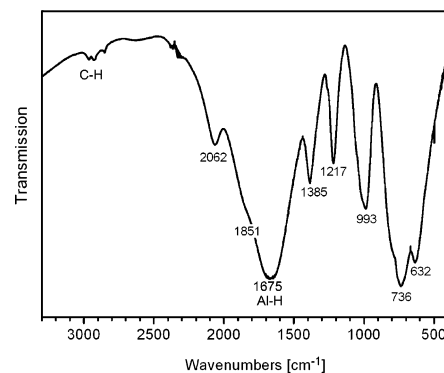


**Figure 2.** IR spectrum of  $\gamma$ -AlH<sub>3</sub>.

The solid was finally transferred to a fine-grade glass filter frit, washed several times with small aliquots of Et<sub>2</sub>O to remove excess LiAlH<sub>4</sub> and any remaining AlH<sub>3</sub>-etherate, and dried under vacuum, yielding 1.5 g (75%) of aluminum hydride.

The material was a nearly pure single phase. The X-ray powder pattern resembled the reference pattern ICDD-PDF #38-0757 for  $\gamma$ -AlH<sub>3</sub> with only a trace amount of LiCl in the material (see Figure 1). The infrared spectra of the samples showed a broad band with a maximum at 1675 cm<sup>-1</sup> in the Al–H stretch region, and only a residual amount of hydrocarbons was detected in the C–H stretch region at 3000 cm<sup>-1</sup>, see Figure 2.

**Instrumentation and Analyses.** Solid-state infrared spectra of the product (as KBr pellets) were recorded in the range of 4000–370 cm<sup>-1</sup> under a nitrogen atmosphere and ambient conditions by using a Perkin-Elmer Spectrum GX FTIR spectrometer. The evaluation was done with the Perkin-Elmer Spectrum, version 2.00, Software.

Powder X-ray diffraction patterns were obtained with a Philips X'PERT diffractometer (Cu K $\alpha$  radiation, 2 kW, with X'Celerator RTMS detector, automatic divergence slit). The powder was measured on a single Si crystal and sealed in the glove box by an airtight hood made of Kapton foil, the foil being mounted out of the focus of the diffractometer. The software for data acquisition and evaluation was X'PERT HighScore 2.2.

**Synthesis at Moscow State University.** Commercial LiAlH<sub>4</sub> was purified by recrystallization from the ether–toluene solution to a purity of 99.3% (these data were obtained by quantitative element analysis, chromatography of the gaseous phase, IR spectroscopy, and XRD). Commercial AlCl<sub>3</sub> was additionally purified by sublimation in a glass ampule above aluminum metal to a purity of

(6) (a) Graetz, J.; Reilly, J. J. *J. Alloys Compd.* **2006**, *424* (1–2), 262–265. (b) Graetz, J.; Reilly, J. J. *J. Phys. Chem. B* **2005**, *109*, 22181–22185.

(7) Turley, J. W.; Rinn, H. W. *Inorg. Chem.* **1969**, *8*, 18–22.

(8) Maehlen, J. P.; Yartys, V. A. In *Advanced Materials for Energy Conversion III*; Chandra, D., Petrovic, J., Bautista, R. G., Imam, A., Eds.; The Minerals, Metals & Materials Society: Warrendale, PA, 2006; pp 77–85.

## Crystal Structure of $\gamma$ -AlH<sub>3</sub>

99.9%. Total content of the transition metals in both initial chemicals was less than  $10^{-3}\%$ . Ether and benzene were purified by boiling and distillation over LiAlH<sub>4</sub>.

$\gamma$ -AlH<sub>3</sub> was synthesized according to the technique described in ref 1 using the reaction  $3\text{LiAlH}_4 + \text{AlCl}_3 \rightarrow 4\text{AlH}_3 + 3\text{LiCl}$  in ether–benzene solution at room temperature. A 12% excess of lithium alanate was used, compared to the stoichiometry. After the reaction was complete, the solution was heated for a distillation of the mixed solvent until the hydride started to crystallize at 75–76 °C. The residual suspension was cooled under Ar gas. Solid  $\gamma$ -AlH<sub>3</sub> was received as thin needles or plates with sizes of  $(1-2) \times (3-5) \times (20-30) \mu\text{m}$ . This product was separated, washed by ether, and dried in a vacuum under slight heating.

**Synchrotron X-ray Diffraction.** SR-XRD studies of  $\gamma$ -alane were performed at the Swiss-Norwegian Beam Line (SNBL, BM1) at the European Synchrotron Radiation Facility (Grenoble). The high-resolution powder diffraction data for  $\gamma$ -AlH<sub>3</sub> was collected at room temperature with the powder diffractometer (in Debye–Scherrer mode) in steps of  $0.003^\circ$  in the  $2\theta$  range from  $4.020$  to  $50.001^\circ$ . Monochromatic X-rays were obtained from a channel-cut Si (111) crystal. For the measurements, the sample was put into a 0.7 mm quartz capillary. The wavelength,  $\lambda$ , selected for the measurements was accurately determined to be  $\lambda = 0.60008(2) \text{ \AA}$  from separate calibration measurements of a standard LaB<sub>6</sub> sample. The Rietveld analysis of the data was carried out using the GSAS software.<sup>9</sup>

## Results and Discussion

The SR-XRD pattern was indexed as an orthorhombic cell with unit cell parameters of  $a = 5.3806(1) \text{ \AA}$ ,  $b = 7.3555(2) \text{ \AA}$ ,  $c = 5.77509(5) \text{ \AA}$ , and volume,  $V = 228.561(7) \text{ \AA}^3$ . The use of the rhombohedral  $\alpha$ -AlH<sub>3</sub> (space group  $R\bar{3}c$  (No. 167) ( $a = 4.44994(5) \text{ \AA}$ ,  $c = 11.8200(2) \text{ \AA}$ ,  $V = 202.701 \text{ \AA}^3$ ) with  $33.78 \text{ \AA}^3/\text{fu}$  of AlH<sub>3</sub><sup>8</sup> for comparison leads to a proposal that the unit cell of  $\gamma$ -AlH<sub>3</sub> contains 6 fu of AlH<sub>3</sub>, yielding a higher value of the molecular volume for  $\gamma$ -AlH<sub>3</sub> ( $38.10 \text{ \AA}^3/\text{AlH}_3$ ) and a smaller value, by 11%, of the density of  $\gamma$ -AlH<sub>3</sub> ( $1.31 \text{ g/cm}^3$ ), compared to that of  $\alpha$ -AlH<sub>3</sub> ( $1.48 \text{ g/cm}^3$ ).

Analysis of the powder diffraction pattern showed that the experimentally observed  $hkl$  indices obey the following extinction rules:  $0kl$ ,  $k + l = 2n$ ;  $h0l$ ,  $h + l = 2n$ ;  $h00$ ,  $h = 2n$ ;  $0k0$ ,  $k = 2n$ ;  $00l$ ,  $l = 2n$ . The latter are consistent with the space group  $Pnmm$  (No. 58). The FOX software package<sup>10</sup> has been used for this space group to determine the structure of the aluminum sublattice. The calculations yielded the positions of Al atoms occupying 2 different sites: 2-fold  $2b$  ( $0,0,1/2$ ) and 4-fold  $4g$  ( $x,y,0$ ;  $x \approx 0.78$ ,  $y \approx 0.08$ ). Even without the location of the hydrogen atoms, the refinement, based on the introduction of 6 Al atoms per unit cell, resulted in a rather good fit:  $R_p = 5.41\%$ ,  $R_{wp} = 6.91\%$ , and  $\chi^2 = 2.63$ .

Anisotropic line broadening of the diffraction pattern was observed and was accounted for in the refinements using the Thompson–Cox–Hastings pseudo-Voigt-type function

(9) Larson, A. C.; van Dreele, R. B. General Structure Analysis System (GSAS), LANSCE, MS-H 805 (1994).

(10) Favre-Nicolin, V.; Cerný, R. *J. Appl. Crystallogr.* **2002**, *35*, 734–743.

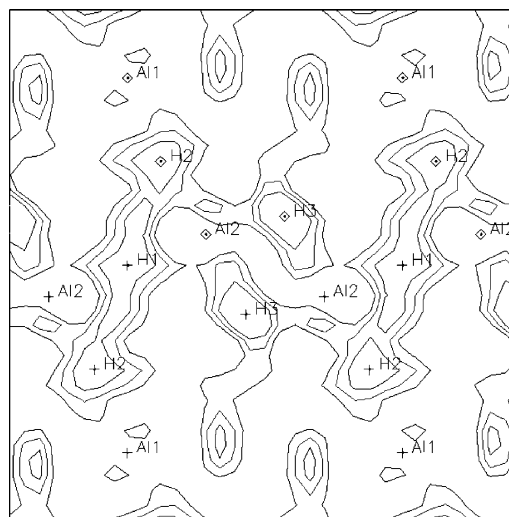


**Figure 3.** Difference Fourier map plotted in the  $x,y$  plane centered at  $x,y,z = (1/2, 1/2, 1/2)$  for  $\gamma$ -AlH<sub>3</sub> showing peaks of electron density associated with the H1, H2, and H3 atoms in the vicinity of Al1 and Al2 (the width of the plot is 10 Å).

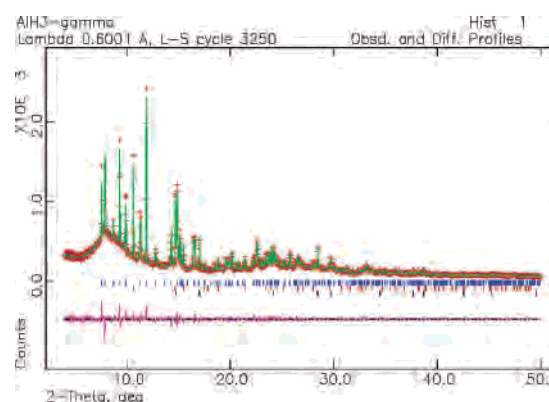


**Figure 4.** Observed (+), calculated (upper line), and difference (lower line) XRD profiles for  $\gamma$ -AlH<sub>3</sub>. Positions of the peaks of the constituent phases are marked (from top to bottom):  $\gamma$ -AlH<sub>3</sub> (83.1(1) wt %),  $\alpha$ -AlH<sub>3</sub> (10.7(1) wt %), and Al (6.2(1) wt %). The secondary phases,  $\alpha$ -AlH<sub>3</sub> and Al, are formed during storage of the initial phase-pure  $\gamma$ -AlH<sub>3</sub> prior to the SR-XRD measurements.

as proposed in ref 11. Size broadening coefficients,  $P$  and  $X$  (describing the Gaussian and Lorentzian contributions, respectively), the mixing coefficient,  $\eta$ , and six microstrain parameters for the orthorhombic system were refined. The values of  $U$ ,  $V$ , and  $W$ , defining instrumental parameters of the measurements, obtained from refinements of a LaB<sub>6</sub> standard, were fixed.

An interesting feature of the Al sublattice is the formation of very short Al–Al distances of  $2.606 \text{ \AA}$  between atoms Al2 and Al2. This feature will be further explained later in the paper, after description of the findings, associated with the most important features of the hydrogen sublattice and Al–H bonding in the structure.

Hydrogen atoms in the structure were located from the difference Fourier synthesis maps allowing identification of 4 different crystallographic sites occupied by 18 H atoms/unit cell. These included H1 ( $2d$   $0, 1/2, 1/2$ ), H2 ( $4g$   $x, y, 0$ ), H3 ( $4g$   $x, y, 0$ ), and H4 ( $8h$   $x, y, 0$ ). Figure 3 shows a

(11) Stephens, P. *J. Appl. Crystallogr.* **1999**, *32*, 281–289.

**Table 1.** Experimental Details and Crystallographic Data for  $\gamma$ -AlH<sub>3</sub>

composition	AlH <sub>3</sub>
fw	30.006
cryst syst	orthorhombic
space group	<i>Pnmm</i> (No. 58)
<i>a</i> (Å)	5.3806(1)
<i>b</i> (Å)	7.3555(2)
<i>c</i> (Å)	5.77509(5)
<i>V</i> (Å <sup>3</sup> )	228.561(7)
<i>Z</i>	6
<i>D</i> (g cm <sup>-3</sup> )	1.308
color	white
temp (K)	293
wavelength (Å)	0.60008
diffractometer	Beamline BM01, SNBL, ESRF, France
data collection mode	Debye–Scherrer
$2\theta$ (deg)	4.020–50.001, increments of 0.003
no. of points	15 327
refinement	
<i>R</i> factors and GOF	$R_{wp} = 0.0614$ , $R_p = 0.0488$ , and $\chi^2 = 2.079$

**Table 2.** Atomic Coordinates and Thermal Parameters for  $\gamma$ -AlH<sub>3</sub>

atom	site	<i>x</i>	<i>y</i>	<i>z</i>	<i>U</i> <sub>iso</sub> (×100 Å <sup>2</sup> )
Al1	2 <i>b</i>	0	0	1/2	1.27(5)
Al2	4 <i>g</i>	0.7875(2)	0.0849(2)	0	0.40(2)
H1	2 <i>d</i>	0	1/2	1/2	2.0(–)
H2	4 <i>g</i>	0.626(4)	0.278(2)	0	2.0(–)
H3	4 <i>g</i>	0.094(2)	0.130(2)	0	2.0(–)
H4	8 <i>h</i>	0.762(2)	0.078(2)	0.309(1)	2.0(–)

difference Fourier map in which the H1, H2, and H3 atoms are clearly seen in the neighborhood of the Al1 and Al2 atoms.

The introduction of hydrogen atoms into the calculations allowed further improvement of the refinement fits. The *R* values decreased to  $R_p = 4.88\%$ ,  $R_{wp} = 6.14\%$ , and  $\chi^2 = 2.08$ . The good quality of the fit of the powder diffraction data is shown in Figure 4. Table 1 summarizes crystallographic data for  $\gamma$ -AlH<sub>3</sub>, and Table 2 gives the atomic coordinates and thermal parameters for  $\gamma$ -AlH<sub>3</sub>.

In  $\gamma$ -AlH<sub>3</sub>, hydrogen atoms form octahedra around Al. Al1 is bonded with two H2 atoms and four H4 atoms, while Al2 is surrounded by H1, H2, two H3, and two H4 atoms (see Figure 5). The Al–H bonding distances in the structure are in the range of 1.66–1.79 Å (Table 3). Despite the rather large variation, they are all close to the only available Al–H binding distance in  $\alpha$ -AlH<sub>3</sub> of 1.712 Å.<sup>8</sup>

The structure of  $\gamma$ -AlH<sub>3</sub> is composed of AlH<sub>6</sub> octahedra, as the building blocks (Figure 6), similar to  $\alpha$ -AlH<sub>3</sub>. However, these octahedra are connected differently, resulting in formation of hydrogen bridge bonds, Al–H–Al, in  $\alpha$ -AlH<sub>3</sub> (Al–H = 1.712 Å, Al–Al = 3.24 Å,  $\angle 142^\circ$ ) or two different types of bridges in  $\gamma$ -AlH<sub>3</sub> (Figure 5), where AlH<sub>6</sub> octahedra of two kinds share vertices and edges. In addition to a normal bridge bond ( $\gamma$  Al–H = 1.65–1.80 Å, Al–Al = 3.17 Å,  $\angle 124.9^\circ$ ), a bifurcated bridge bond between two aluminum and two hydrogen atoms is formed. The geometry of this bond (Al–H = 1.68 and 1.70 Å,  $\angle 100.7^\circ$ ) allows for a close proximity between aluminum atoms Al–Al = 2.606 Å. This appears to be even shorter than the Al–Al distances in Al metal (2.86 Å).

The formation of the bifurcated double-bridge bond, Al–2H–Al, is a prominent feature of the crystal structure of

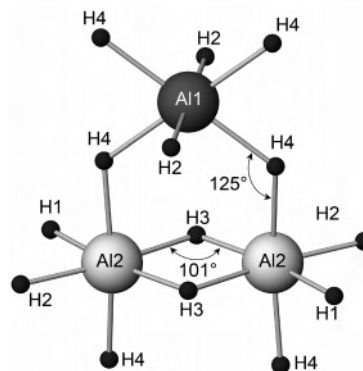


**Figure 5.** Two types of the available AlH<sub>6</sub> octahedra, Al1H<sub>2</sub>H<sub>4</sub> and Al2H<sub>1</sub>H<sub>2</sub>H<sub>3</sub>H<sub>4</sub>, and their interconnection in the crystal structure of  $\gamma$ -AlH<sub>3</sub>. A double-bridge bond, Al2–2H3–Al2, and one type of the bridge bond Al1–H4–Al1 are shown. For Al1, all Al–H distances are large (1.78–1.79 Å). For Al2, the axial bonds, Al–H = 1.78 Å, are as long as the Al1–H distances. However, H atoms participating in the double-bridge bonds, H–2Al–H, form much shorter bonds with Al (1.68 and 1.72 Å). This proximity results in a short interatomic distance between two Al2 atoms of only 2.606 Å and a much lower bond angle (101°) than the normal bridge bond angle of 125°.

**Table 3.** Selected Interatomic Distances (Å) and Bond Angles (deg) in the Crystal Structure of  $\gamma$ -AlH<sub>3</sub><sup>a</sup>

atoms	distances	atoms	distances	atoms	angles
Al1–4Al2	3.1679(4)	Al2–H1	1.668(1)	Al1–H4–Al2	124.9(6)
Al1–4H4	1.784(6)	Al2–H2	1.664(8)	Al1–H2–Al2	171.0(2)
Al1–2H2	1.769(8)	Al2–H3	1.68(1)	Al2–H1–Al2	180.0(–)
Al2–2Al1	3.1679(4)	Al2–H3	1.70(1)	Al2–H3–Al2	100.7(7)
Al2–Al2	2.606(2)	Al2–2H4	1.790(8)		

<sup>a</sup> All H–H distances in the structure exceed 2.1 Å.

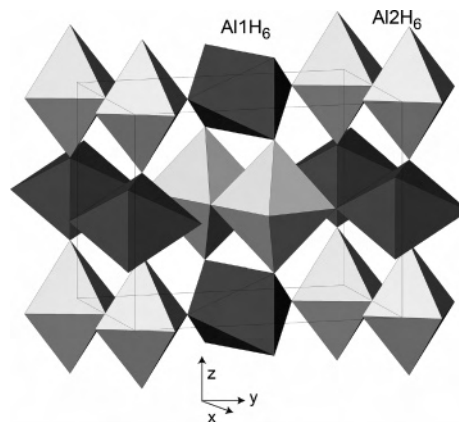


**Figure 6.** Framework of the AlH<sub>6</sub> octahedra in the crystal structure of  $\gamma$ -AlH<sub>3</sub> showing interconnection between two types of the available AlH<sub>6</sub> units, Al1H<sub>6</sub> and Al2H<sub>6</sub>. Octahedra are connected by vertices (Al1H<sub>6</sub>–Al2H<sub>6</sub>) or by edges (Al2H<sub>6</sub>–Al2H<sub>6</sub>). This results in the formation of normal bridge bonds, H–Al–H, or double-bridge bonds, Al–2H–Al (latter).

$\gamma$ -AlH<sub>3</sub>. This feature is unique for the Al-containing hydrides and has not been previously reported for its hydrides.

Indeed, the AlH<sub>6</sub> octahedra are frequently found in the crystal structures of Al-containing hydrides. They exist either as AlH<sub>6</sub><sup>3–</sup> ions or as covalently bound neutral AlH<sub>6</sub> polyhedra. The AlH<sub>6</sub><sup>3–</sup> ions are present as isolated units in the structures of the R<sub>3</sub>AlH<sub>6</sub> hexahydrides, for example, in Na<sub>3</sub>-AlH<sub>6</sub>,<sup>12</sup> K<sub>2</sub>LiAlH<sub>6</sub>, and K<sub>2</sub>NaAlH<sub>6</sub>.<sup>13</sup>

(12) Ronnebro, E.; Noreus, D.; Kadir, K.; Reiser, A.; Bogdanovic, B. *J. Alloys Compd.* **2000**, *299*, 101–106.

### Crystal Structure of $\gamma$ -AlH<sub>3</sub>

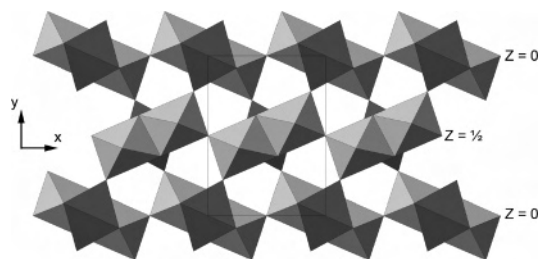


**Figure 7.** Projection of the crystal structure of  $\gamma$ -AlH<sub>3</sub> along [001] shown as a packing of the AlH<sub>6</sub> octahedra. Large cavities in the structure are clearly seen.

On the other hand, AlH<sub>6</sub> octahedra share vertices in the crystal structure of  $\alpha$ -AlH<sub>3</sub>,<sup>8</sup> thus, forming normal bridge bonds, Al–H–Al. Such bonds are a consequence of the electron deficiency of the elements of the third group, which may self-stabilize by the formation of 3-center 2-electron bridge bonds in the case of covalent compounds.

Finally, one additional feature of the crystal structure of  $\gamma$ -AlH<sub>3</sub> should be mentioned. This feature lies in the formation of large cavities between the AlH<sub>6</sub> octahedra. The cavities are clearly seen in the Figure 7. The vertices of a set of two edge-connected Al<sub>2</sub>H<sub>6</sub> octahedra are always connected to two other pairs of edge-connected Al<sub>2</sub>H<sub>6</sub> octahedra and to four single vertex-connected AlH<sub>6</sub> octahedra. Hence, the strands of Al<sub>2</sub>H<sub>6</sub> are always separated by single AlH<sub>6</sub> octahedra, which are differently oriented in space. As a result of such packing, the structure of  $\gamma$ -AlH<sub>3</sub> has a much smaller, by 11%, density than  $\alpha$ -AlH<sub>3</sub>.

The decomposition reaction enthalpy of  $\gamma$ -AlH<sub>3</sub> is 7.1 kJ/mol,<sup>6</sup> which is small, compared to that one of  $\alpha$ -AlH<sub>3</sub> which is 11.4 kJ/mol.<sup>6</sup> In the case of AlH<sub>3</sub>, the reaction enthalpy is the same as the enthalpy of formation because the products are elements; therefore, the average binding energy in  $\gamma$ -AlH<sub>3</sub> is lower than that in  $\alpha$ -AlH<sub>3</sub>. Since the (thermodynamic) decomposition temperature and the equilibrium pressure is related to the Gibbs free energy, this should make a contribution to lower the decomposition temperature of the  $\gamma$ -modification. A different contribution comes from the reaction entropy, which should be lower in the case of the  $\gamma$ -compound, if the assumption of a higher degree of disorder in the  $\gamma$ -phase is justified. At equilibrium ( $\Delta G = 0$ ), the Gibbs equation can be written as

$$T_{\text{eq}} = \frac{\Delta H}{\Delta S} \quad (1)$$

Thus, both the numerator and denominator decrease in eq 1 when changing from the  $\alpha$ - to  $\gamma$ -phase. However, because the equilibrium pressure of the  $\gamma$ -AlH<sub>3</sub> is higher and the decomposition temperature is lower, this indicates a dominating effect of the average binding energy,  $\Delta H$ , over the entropy.

**Acknowledgment.** This work has received support from INTAS Project 05-100005-7665 “New Alane. Novel Reversible Hydrogen Storage Materials Based on the Alloys of Al” and from the HGF initiative “FuncHy”. We thank ESRF and SNBL for provision of beam time.

**Supporting Information Available:** Crystallographic data in CIF format. This material is available free of charge via the Internet at <http://pubs.acs.org>.

IC0617487

(13) Graetz, J.; Lee, Y.; Reilly, J. J.; Park, S.; Vogt, T. Structures and thermodynamics of the mixed alkali alanate. *Phys. Rev. B*, **2005**, *71*, 184115.